MEDICAL PHYSICS PUBLISHING

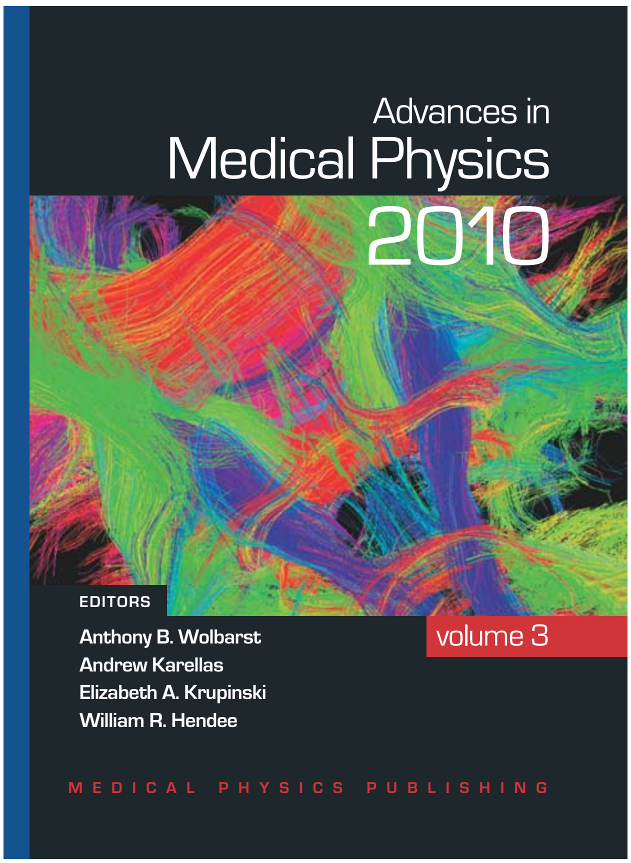

Here is a sample chapter from this book.

CHAPTER 5

Robotic Systems for MRI-Guided Interventions

*Eftychios G. Christoforou, Ph.D.[1] and Nikolaos V. Tsekos, Ph.D.[2]**
[1]KIOS Research Center, University of Cyprus, Nicosia, Cyprus
[2]Medical Robotics Laboratory, Department of Computer Science, University of Houston, Houston, Texas

* Corresponding author.

5.1 Introduction

Two important new developments in modern medicine have been image-guided interventions (IGI) and minimally invasive surgery (MIS). They have already brought about improvements to patient treatment and, eventually, may lead to greater overall cost-effectiveness. A promising aspect of both is the emergence of robotic systems [e.g., Goh et al. (1993); Boyd et al. (1992); Nathoo et al. (2005); Reijnen et al. (2005); Menciassi et al. (2007); Taylor and Jayne (2007); Anderson et al. (2008) and references therein]. With applications in orthopedics, neurosurgery, thoracic surgery, and other areas, these systems capitalize on features inherent to robots, including remote-presence, accuracy, motion/force scaling, and a steady hand. Also, robotics frequently incorporates innovations in other high-tech fields such as imaging, information technology, and communications.

Recently, the application of robotics for the performance of interventions under magnetic resonance imaging (MRI) guidance has received particular attention, and robots have been designed specially for this purpose. Because of certain properties unique to this modality, reviewed in Tables 5–1 and 5–2, and an ever-growing number of innovative technological and methodological advances, MRI has emerged as a strong candidate for planning, guiding, and monitoring interventions (Tsekos et al. 2007; Gassert et al. 2008a,b). MRI offers a number of soft-tissue contrast mechanisms that allow for the assessment of both anatomical morphology and function (Jolesz et al. 2001a,b); contrast mechanisms such as those that underlie magnetic resonance angiography (MRA), functional MRI (fMRI), and diffusion tensor imaging (DTI) provide methods for comprehensive diagnosis and characterization of tissue pathophysiology, as well as for the delineation of targets in guiding interventions. MRI is also an intrinsically three-dimensional (3D) modality that allows unrestricted selection of oblique 3D or multislice imaging, and scanners allow dynamic "on-the-fly" adjustment of the imaging (Atalar et al. 1998; Zhang et al. 2000, 2001; Hillenbrand et al. 2004; Karmarkar et al. 2004; Wacker et al. 2005; Christoforou et al. 2007). This feature can be used to follow the movement of an MR-compatible interventional robotic device dynamically, thereby allowing freehand dynamic guidance and control of the procedure in a way similar to hand-held ultrasound (Christoforou et al. 2007). An important feature of MRI, pertinent to IGI, is that the quality of images is less dependent on the hands-eye coordination and experience of the operator than for ultrasound-guided interventions.

Limited access to patients inside an MRI scanner, on the one hand, and potential benefits of real-time image guidance, on the other, have led to the introduction of several robotic systems for performing MRI-guided interventions (Tsekos and Jayne 2007: Gassert et al. 2008a,b). The use of MR-compatible robots has been demonstrated in applications including neurologic procedures (Masamune et al. 1995; Sutherland et al. 2008; Pandya et al. 2009), breast interventions (Kaiser et al. 2000; Felden et al. 2002; Larson et al. 2004), endoscope manipulation (Koseki et al. 2002), and prostate procedures (Susil et al. 2003, 2004; Krieger et al. 2005; Zangos et al. 2007). General-purpose systems have also been developed for use with standard cylindrical MR scanners (Hempel et al. 2003; Tsekos et al. 2005, 2008; Melzer et al. 2008). With those systems, various diagnostic and therapeutic procedures have been tested, including studies on patients such as biopsies, aspirations, percutaneous local drug delivery, and ablations.

Table 5–1. *From "MRI-guided interventions" to "robot-assisted MRI-guided interventions"*

MRI for Guiding Interventions and Surgeries
Numerous contrast mechanisms for anatomical and functional information
True 3D and multislice 2D
Computer control of imaging parameters on-the-fly
No ionizing radiation
MRI-Guided Robot-Assisted Interventions and Surgeries
Access to the patient inside the MRI scanner (esp. high-field cylindrical scanners)
Real-time imaging for guidance and response to adjust the procedure
Generic robot features (e.g., accuracy, stability, tremor filtering, etc.)

5.2 MRI-Guided Robot-Assisted Interventions

5.2.1 The Environment

MRI affords unparalleled visualization capabilities, but it also imposes two major challenges when considered for guiding interventions. The first is the presence of three types of strong magnetic fields—the static, principal field; rapidly changing gradients; and radiofrequency (RF) fields. Materials and devices must therefore meet certain MR compatibility and safety criteria, which will be discussed in the following sections. The second obstacle is the limited access to the patient inside the scanner, Figure 5–1. The degree of accessibility varies among the existing scanner types. The best is provided by *open* MR scanners, which consist of two parallel magnet pole faces typically 40 to 45 cm apart, so that there is sideways access to the patient. Open scanners operate at low magnetic fields in the range of 0.02 to 0.7 Tesla (T)

Table 5–2. *Methodological and technical features of MRI and their application in robot-assisted interventions*

Feature	Application
Multi-contrast	Complementary pathophysiologic information for: • pre-operative path planning *and* • intraoperative monitoring (e.g., ablations)
Endogenous "absolute" coordinate system of the MR scanner	Registration of the robotic manipulator Forward kinematics calculations Multi-contrast image co-registration Stereotactic planning
Surface RF coils	High SNR for a specific volume of interest (example, the targeted area as in Figure 5–5)
True 3D or multislice 2D *and* arbitrary definition of imaging planes/volumes	Stereotactic planning based on 3D data Automatic or semiautomatic determination of access corridors: automatic alignment or image-based manual guidance
On-the-fly adjustment of imaging planes and/or contrast mechanism	Manipulator-driven control of imaging parameters to follow the end-effector
Freehand (manual) control of the robotic manipulator and automated forward-looking	Interactive adjustment of the acquisition strategy as needed during the procedure
Fast (sub-second) MR imaging	On-the-fly adjustment of the procedure Motion tracking for compensation
Miniature passive or active MR markers	Visualization of tools in MR images Initial registration of the robotic manipulator MR-based calculation of spatial position for position validation and closed-loop control

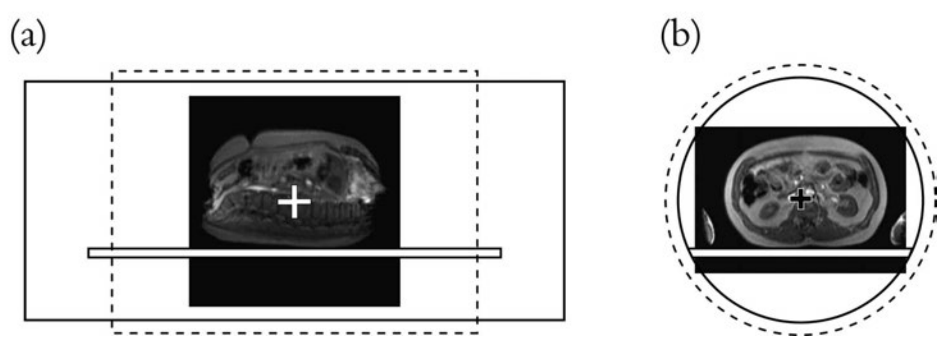

Figure 5–1. Patient accessibility in high magnetic field cylindrical MR scanners is limited. The images are sagittal and transverse slices through the abdomen, collected with an FOV = 50×50 cm^2. The solid-line box and circle correspond to the inside limits of the gantry of an MR scanner that is 180 cm long and 60 cm wide. The dotted box and circle correspond to a newer generation of shorter and wider scanners with a length of 120 cm and a gantry diameter of 70 cm. Although the latter designs offer more space above the patient and shorter distance to reach, direct manual access is still not possible; robotic systems can both provide direct patient access and facilitate an intervention with real-time MR guidance.

and more recently up to 1 T. Alternatively, a *split bore* (or "double-donut") scanner consists of two adjacent and collinear magnets that allow direct access to the patient from the opening between them, which is about 50 cm wide. However, double-donut scanners are no longer commercially available. In clinical practice most scanners use cylindrical superconductive magnets, with the diameter of the bore typically 60 cm (although a 70-cm wide scanner is also commercially available) and the length ranging from 1.20 to 2.0 m. Such cylindrical scanners operate at 1.0 to 3.0 T and offer the best available signal, field homogeneity, and speed of image acquisition.

The current practice of performing MRI-guided procedures with cylindrical scanners is primarily based on pre-operative MR image information, and most applications involve needle targeting. The actual interventional tasks are performed outside the scanner, but multiple entries back into it may be required for identification of the targeted anatomy and for the correct placement of MR-visible fiducial markers for localization. After the insertion of an interventional tool, for example, a new image acquisition follows to validate the correctness of its placement; then the patient is removed from the scanner to complete the procedure (e.g., harvest a biopsy sample). A major weakness of the approach is that because the anatomical information is not updated intraoperatively, any tissue shifts induced by the advancement of the interventional tools cannot be compensated for at the time. Tissue displacements due to the advancement of the interventional tool are difficult to predict, as they depend on tissue elastic properties and on the speed of tool advancement (Debatin et al. 1998; Pfleiderer et al. 2003, 2005; Susil et al. 2003, 2004; Krieger et al. 2005). Moreover, the specific interventional approach becomes lengthy and causes additional discomfort to the patient. It may also cause more surgical trauma and increased chances for complications due to subsequent insertion attempts (Lufkin et al. 1999).

MR-compatible manipulators have been proposed (Tsekos et al. 2007; Gassert et al. 2008a,b) to provide the required access to the patient inside the scanner and to allow real-time guidance and monitoring of procedures. Robotic technology provides the means to perform IGI in cylindrical scanners and, therefore, effectively exploits their superior imaging capabilities compared to open scanners. With robotic systems, targeting and monitoring of a procedure can be performed while the patient remains inside the scanner, largely eliminating the need for cumbersome multiple reentries.

5.2.2 Integration of MRI and Robotics

MRI has emerged as a one of the most versatile modalities for planning, guiding and monitoring, due largely to the unique properties reviewed in Tables 5–1 and 5–2 (Tsekos et al. 2007; Gassert et al. 2008a,b). Apart from those specific properties and concomitant benefits, modern MRI scanners are endowed with a wealth of technical innovations that exploit the specific way that the signal is spatially encoded to generate images (i.e., phase encoding with magnetic field gradients). The ability to electronically control, even on-the-fly (Atalar et al. 1998; Zhang et al. 2000, 2001; Hillenbrand et al. 2004; Karmarkar et al. 2004; Wacker et al. 2005; Christoforou et al. 2007), the imaging parameters presents a unique opportunity for integrating the MRI scanner, the *robotic manipulator*, i.e., the arm and the *end-effector* at its distal end that carries, typically, an adjustable "hand" or other instruments, and the operator, together in a seamless cyber-physical system. Figure 5–2 illustrates a possible scheme for integrating these three components into a single system. The interaction of the operator with this system is based on both *haptic* and visualization interfacing. (*Haptics* technology allows control by, and feedback to, the operator based on the sense of touch.) To discuss the

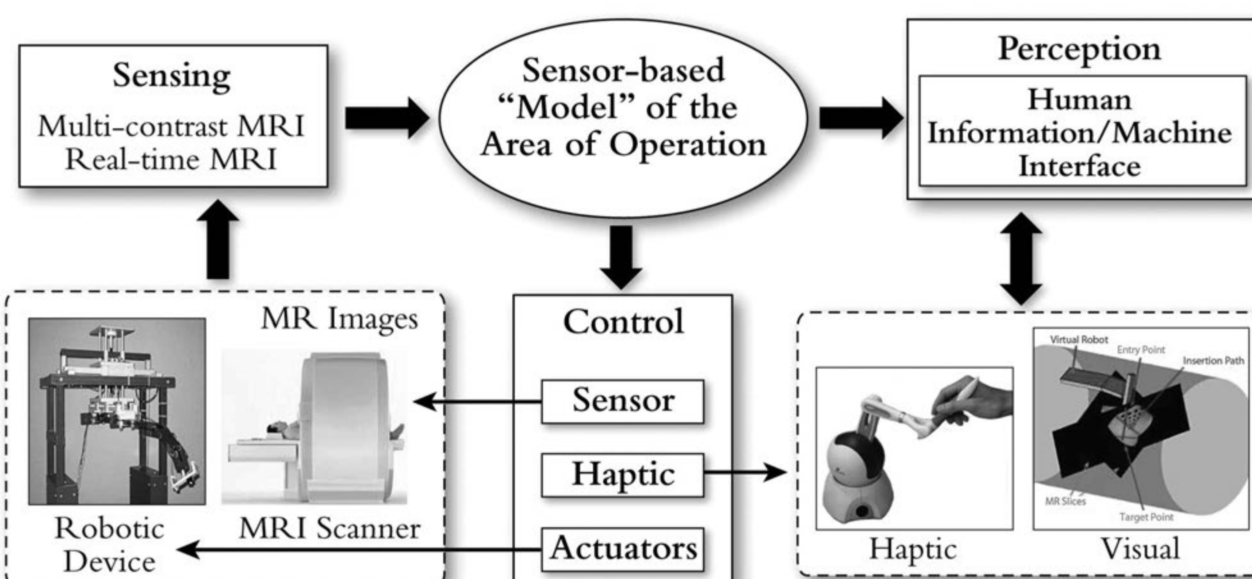

Figure 5–2. An information system for performing MRI-guided robot-assisted interventions integrates four interconnected elements: Sensing, Modeling, Control, and Perception. The block arrows illustrate the flow of data from the scanner to the computational code, as well as the flow of information toward the operator, and the solid arrows indicate the control flow. Since MRI can offer a wide range of soft-tissue contrasts that, in most cases, can be collected and updated intraoperatively, it offers the opportunity to use data to generate a true-"model" of the Area of Operation that is updated on-the-fly. As such, MRI that is integrated into the procedure is an information system rather than just a mere scanner.

integration of robotics and MR guidance, we will use a didactic paradigm based on a prototype developmental platform used to develop and investigate different enabling-technologies and approaches for performing robot-assisted interventions with MR guidance (Tsekos et al. 2005; Christoforou et al. 2007; Karanikolas et al. 2006; Ozcan et al. 2006; Ozcan and Tsekos 2008). Figure 5–3 illustrates the architecture, the processes and the flow of information of this system.

The control component comprises routines that are called by the other components of the computational core of the system, on a per-need-basis, to calculate *forward* and *inverse kinematics* of the manipulator. Forward kinematics describes the end-effector (end-tool) position and, given the specific values of the joints; inverse kinematics provides the joint values for a given position of the end-effector. All kinematic calculations for MRI-guided robot control are performed relative to the coordinate system of the MR scanner. The ability to register a point of any entity (patient, robot, tools, etc.) relative to this coordinate system is a major benefit, and a property inherent to the tomographic modalities of both MRI and CT.

Registration of the position of the manipulator can be achieved using MR-visible passive (Tsekos et al. 2005) or active (Zhang et al. 2000; 2001; Hillenbrand et al. 2004) fiducial markers. Figure 5–4 shows the appearance of a two-dimensional (2D) cross-shaped marker on a robot (Tsekos et al. 2005). Since the positions of the markers are known relative to the robotic structure, the initial position of the manipulator relative to the coordinate system of the MR scanner is determined. Knowing the initial position of the robot and the original set of the *degrees of freedom* (*DOF*) values, the forward and inverse kinematics can then be calculated relative to the MR scanner coordinate system.

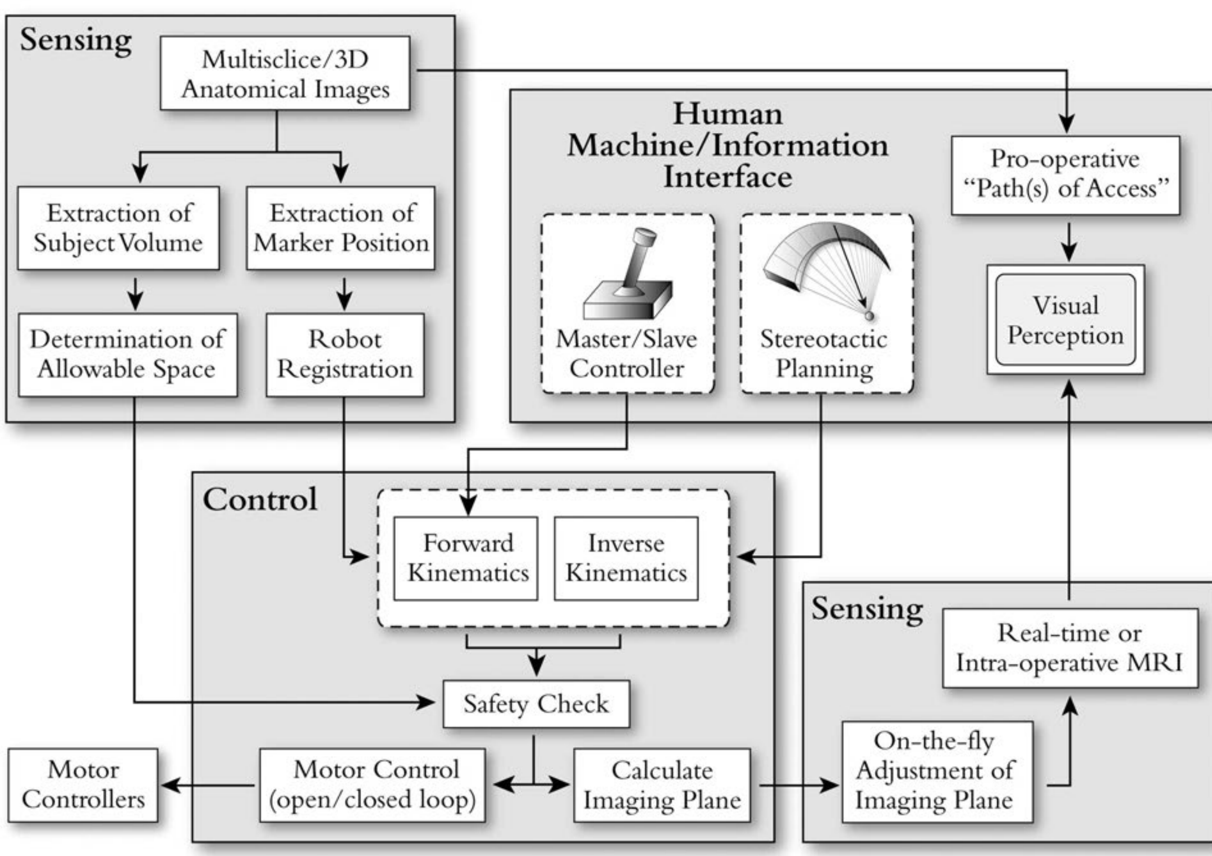

Figure 5–3. The processes and flow of information for an example of MR image-based interventional robot control software [as implemented with the robotic system in Tsekos et al. (2005)]. The three interrelated elements of sensing, control, and perception are delineated with the boxes shaded in gray; unlike Figure 5–2, this system does not include modeling or haptics. The robot is registered relative to the coordinate system of the MR scanner. From multislice anatomical MR images, the software determines the "Allowable Space" inside the MR scanner for use by the Safety Check routine, to prevent collisions of the robot with the subject. The registration information is used also by both the forward and inverse kinematics (dotted line box). The operator uses either stereotactic or "freehand" master/slave control. In the former case, the inverse kinematics equations are solved to determine the appropriate set of DOF values, as well as their compliance with the safety routine. In the latter, the forward kinematics equations yield the coordinates of the requested final position; this kinematic configuration of the robot is then tested for compliance with the safety routine, and it is executed only if the requested motion is within the allowable space. With the freehand control method, the operator manually adjusts the robot.

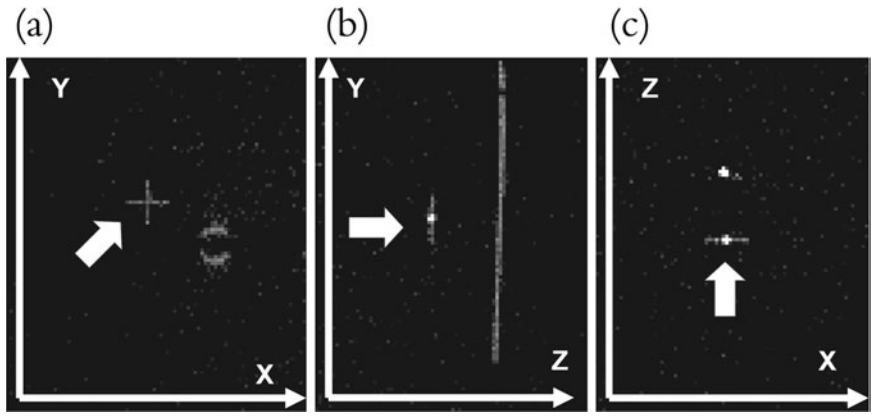

Figure 5–4. An important issue in robotic interventions is the co-registration of patient, robot, and visualization modality. MR offers a feature unique to the modality: a coordinate system of reference on which all images are spatially encoded. Using fiducial markers such as the 2D cross-shaped marker depicted in this figure and pointed out with the white arrow, the robot can also be registered to this coordinate system. With such markers, the coordinates of the center of a cross can be extracted: from a transverse slice (a) the coordinates X and Y, from a coronal slice (b) the Y and Z, and the Z and X from a sagittal slice (c). The redundant values can be averaged or, alternatively, any pair of them can be accepted. These coordinates can then be used in the kinematics calculations of the robotic system. Registration may occur once at the beginning of an intervention, or be repeated whenever necessary.

The control component incorporates an autonomously and continuously running safety routine that prevents any moving part of the manipulator from colliding with the subject or the gantry of the scanner (Tsekos et al. 2005; Christoforou et al. 2007). This feature has authority over any other process that may alter the configuration of the manipulator. That is, any instruction is first validated by this routine before it is carried out. This is an image-based process: after the initial registration of the robot, a multislice set is collected; the outside surface of the patient is then extracted and interpolated to a 3D surface in the coordinate system of the MR scanner. Then, the space between this surface and the gantry of the scanner defines the *allowable space*, i.e., the space where the manipulator can safely maneuver. After a motion instruction is approved, this routine is used to generate the appropriate motor control commands. The control component can also send instructions to the MR scanner itself, Figure 5–3 (Christoforou et al. 2007).

The latter process is the link between the robot and the scanner that completes the seamless loop between perception, control, and sensing, Figure 5–2. When activated, this routine uses as input the same control instructions sent to the manipulator to calculate the motion of its end-effector relative to the coordinate system of the MR scanner. This information is then sent to the MR scanner for on-the-fly adjustment of the orientation of the imaging planes (Christoforou et al. 2007). The dynamic control of image acquisition parameters allows their adjustment during imaging, permitting us to optimize the procedure as it evolves. Figure 5–5 illustrates the power of MRI to manipulate electronically the way data are collected. In this study, the acquisition of an oblique multislice set of planes offers a dynamic volumetric perspective of the area of interest.

5.3 MRI-Based Guidance

5.3.1 Stereotactic MRI-Based Guidance

Stereotactic guidance and autonomous or semi-autonomous control of the robotic manipulator are used, in some form, in most MR-compatible systems. The process begins with the visual inspection of pre-operative MR images to define a path for the insertion of the interventional tool; this involves selecting the targeted lesion as well as a skin point of insertion (i.e., defining the insertion vector). The robotic system is then instructed to automatically align its end-effector with the prescribed insertion vector. For this purpose, the system employs the inverse kinematics solution and an appropriate path planning algorithm. Since the manipulator is registered to the MR scanner, and the patient does not change position, the robot can autonomously and accurate align its end-effector along the desired trajectory selected by the operator from MR images. With an MRI-guided robot, there is no need to re-register the images and/or the patient to the stereotactic system. With MRI, the operator may also use images with different contrast to assess different anatomical and pathological features, thereby defining the most appropriate approach to the targeted anatomy.

The prototype system described here can perform stereotactic guidance (Tsekos et al. 2005; Christoforou and Tsekos 2006; Ozcan and Tsekos 2008). Upon approval of a path by the operator, the safety routine checks the appropriateness of all involved motions, ensuring that no collision will occur for any transient position of the manipulator. The control component of the core software actuates the DOF of the manipulator to position the end-effector such that the axis of this interventional tool is aligned with the selected path.

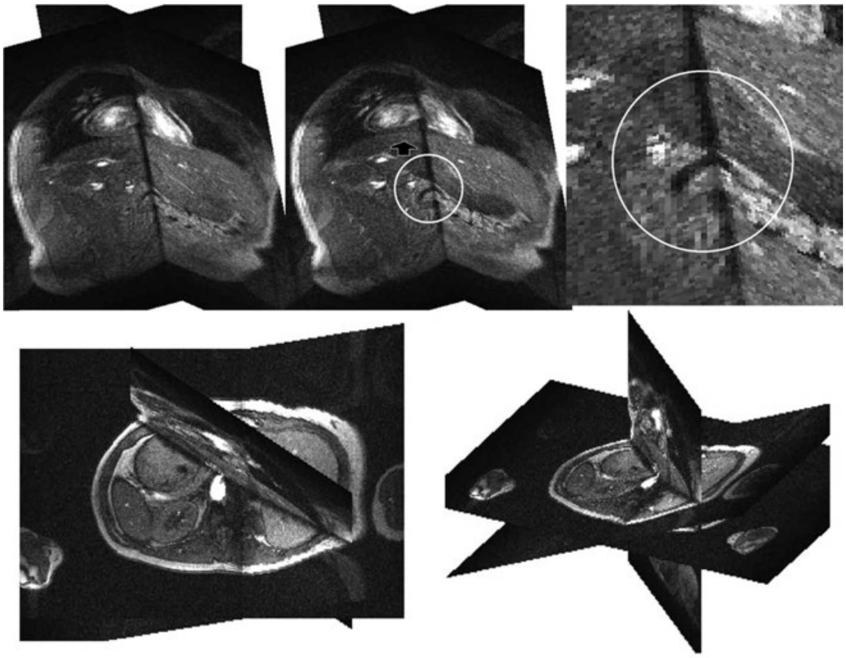

Figure 5–5. In modern MR scanners, rapid repetitive acquisition of multiple planes provides a dynamic perspective of the area of operation. The upper panel shows two consecutive frames from a dynamic series; each is composed of two oblique-to-each-other slices through the abdomen. Note the accurate matching of the anatomical structure boundaries (especially in the zoomed-in third image in the top row). The lower panel shows two perspectives of a frame from another dynamic MR study composed of three slices through the abdomen. From such dynamic multislice sets, the operator can monitor on-the-fly the robot, the targeted anatomy, and other aspects of interest.

Issues of misalignment of needle path with the targeted tissue (due to motion, tool bending, or tissue displacement) must be addressed. The option for direct operator control can address this issue while the operator can use the manual Master/Slave control device to effectively correct the needle trajectory (in a similar manner with that shown in Figure 5–6a). Note that the stereotactic strategy shown in Figure 5–6b is appropriate to achieve accurate target alignment only with non-moving tissue, for example, in neurosurgical procedures.

5.3.2 Freehand Control and MRI-Based Guidance

Stereotactic guidance combined with the anatomical and functional information offered by multi-contrast MRI is a powerful tool for numerous kinds of interventions. Moreover, recent technological innovations available for the state-of-the-art MRI scanners offer intriguing opportunities such as performing procedures with the operator manually controlling, on-the-fly, both the robotic manipulator and the MR scanner simultaneously. Modern MRI scanners offer this capability by means of interactively adjusting the imaging planes, in ways that resemble moving an ultrasound probe to scan the area of interest, or shifting the camera attached to one of the arms of the da Vinci® endoscopic system. With MRI, a manually or "freehand"-controlled manipulator can interface to a scanner, allowing on-the-fly adjustment of imaging parameters, including the position and orientation of imaging slices, in a straightforward computer-controlled manner. This capability was initially demonstrated in vascular MRI-guided interventions, and used for on-the-fly adjustment of MRI imaging parameters to follow the movements of a catheter dynamically (Atalar et al. 1998; Zhang et al. 2000, 2001; Hillenbrand et al. 2004; Karmarkar et al. 2004; Wacker et al. 2005).

Recently, Christoforou et al. (2007) demonstrated the integration of the prototype MR-compatible robotic manipulator discussed herein with a commercial MRI scanner. The instantaneous position of the robot is sent to the controller of the MR scanner, which immediately adjusts the position and orientation of the imaging plane to visualize the end-effector. This mode allows the operator to maneuver the end-effector above the area of interest while scanning the anatomy, Figure 5–7. Operator control of the interventional tool and rapid updating of the imaging plane together yield a simple and intuitive image guidance system similar to that of ultrasound-guided interventions or endoscopy-based surgical robots. The manipulator-driven real-time imaging provides for scouting the subject, identifying a target, and setting the path of the interventional tool to clear for obstacles and align it to the target. Man-in-the-loop image-guided control may also provide the means to practice the compensation of needle bending, a major source of error observed in previous studies with MR compatible systems error (Pfleiderer et al. 2003, 2005; Susil et al. 2003, 2004), since the operator can use dynamic imaging to appropriately react to and correct the bending. Having the tool always at the same position and orientation relative to the field of view (FOV) provides a straightforward way of directing it, while a simple software routine can place a line-of-sight on any frame without any special image processing. Figure 5–7 illustrates an example of manual control of the robot using real-time MR images with simple graphical objects overlaid to assist manual control with visual input.

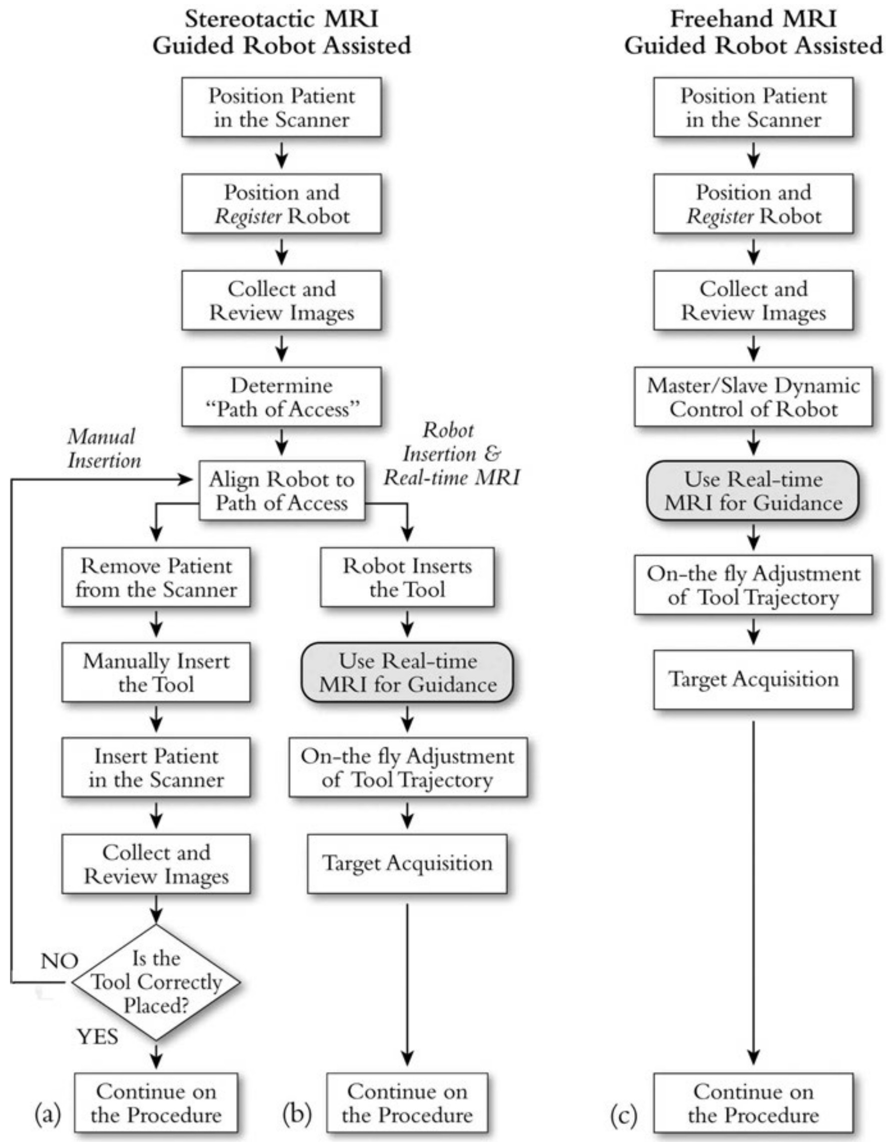

Figure 5–6. The steps and processes involved in the performance of stereotactic (a and b) and freehand (c) MRI-guided procedures, with the integrated robotic system of Figure 5–3. In (a), the robot aligns the interventional tool along the desired trajectory, but the insertion is performed manually after removing the patient from the scanner; this practice increases both the duration of the procedure and the chance of missing the target due to tissue displacement. In (b) and (c), the man-in-the-loop strategies allow the operator to directly alter the path of insertion during dynamic imaging (see Figure 5–7). The benefit of a robotic system with real-time image guidance is evident.

5.4 Mechatronics

5.4.1 Compatibility with MRI Scanners

Similar to any other medical instruments intended for clinical use, MR-related devices are required to meet strict criteria and to obtain prior approvals by regulatory agencies. The development of MR-compatible devices faces critical challenges, mainly those presented by high magnetic fields, strong and fast-switching magnetic field gradients, and radiofrequency pulses. MR compatibility is concerned with the behavior of an object inside the scanning environment as well as the effect of the object on image acquisition. For example, devices or interventional tools coming near the magnet cannot contain ferromagnetic materials, which are subject to strong magnetic forces (Schenck 1998, 2000; Shellock and Crues 2004), and also their presence alters the homogeneity of the main magnetic field resulting in susceptibility artifacts. Another MR compatibility issue is the sensitivity of the imaging acquisition to electromagnetic noise resulting in deterioration of the image signal-to-noise ratio (SNR). For isolation purposes, entire scanner rooms themselves are highly shielded Faraday cages. This sensitivity is a major concern regarding the noise originating from electronic components of any mechatronic interventional device required to reside inside the scanner room. Moreover, wiring that enters the scanner room from outside may also play the role of an antenna radiating noise.

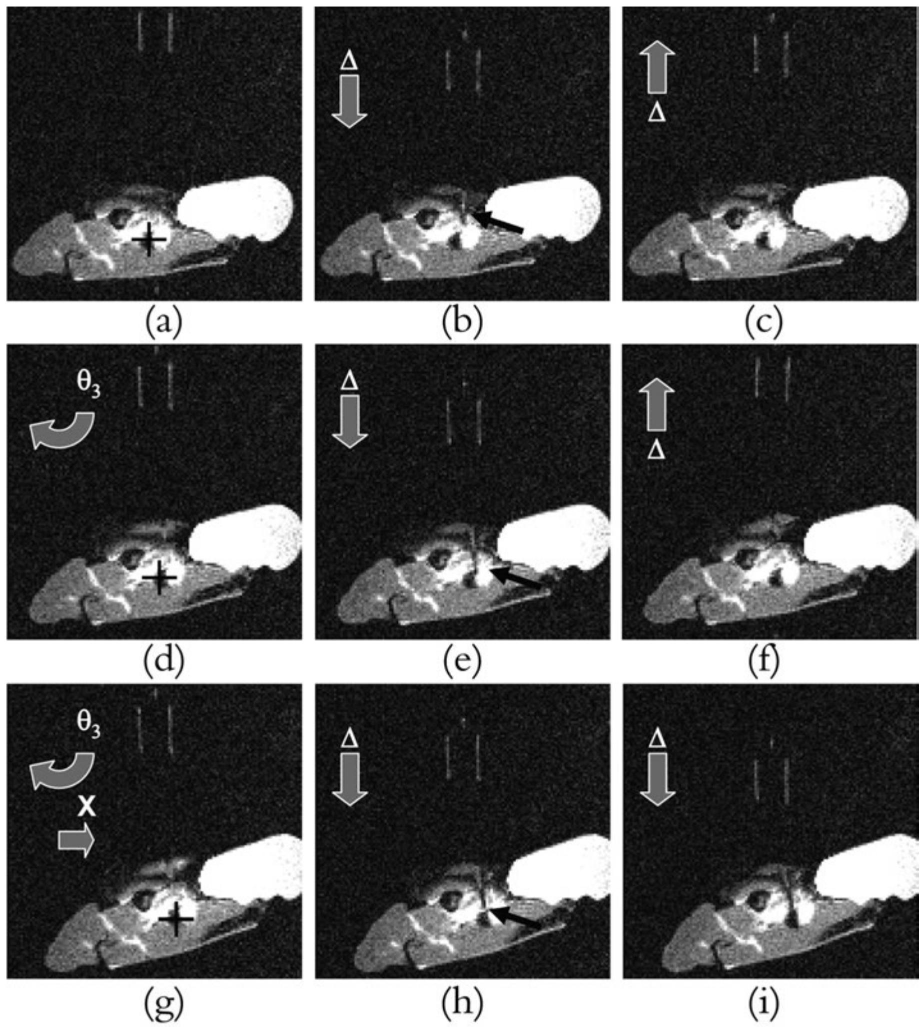

Figure 5–7. Selected frames from a study using the freehand master/slave control method of Figure 5–6c, with direct on-the-fly adjustment of the imaging plane to always include the end-effector (delineated by the two parallel gadolinium-filled tubes). These studies were performed with the manipulator described in Tsekos et al. (2005). In these studies the robot was manually controlled via a master-slave control handle (Christoforou et al. 2007). Here, the operator performed three consecutive insertions of an MR-compatible needle into a target (identified by the cross), simulating on-the-fly adjustment of the needle trajectory to compensate for needle bending. In the first insertion (b), the trajectory of the needle (black arrow) will miss the target, so the operator removes it (c), rotates slightly (d), and then re-inserts it (e). The new trajectory is closer to the target, but still not on it, so the needle is withdrawn again (f). A farther rotation (g) causes enough bending of the needle to achieve the desired targeting, (h) and finally (j). This set depicts nine out of over 300 hundred frames collected during the maneuvers. (Adapted from *Magn Reson Imaging,* "Performance of interventions with manipulator-driven real-time MR guidance: implementation and initial in vitro tests." E. Christoforou, E. Akbudak, A. Ozcan, M. Karanikolas, and N. V. Tsekos, vol. 25, issue 1, pp. 69–77. © 2007, with permission from Elsevier.)

The literature agrees, in general terms, about the definitions of MR safety and compatibility of an object or device [e.g., FDA (1997); Jolesz et al. (1998); Keeler et al. (1998); Schenck (1998, 2000); Shellock (2000); Chinzei and Miller (2001); Tsekos et al. (2001); Larson et al. (2004); Shellock and Crues (2004)]. A device is considered to be MR-safe inside the MR environment when it does not present any additional risk to the patient. The effect of the device on image quality is normally not considered as a safety issue (i.e., an MR-safe device may still affect the quality of the images). The compatibility definition states that for an object to be MR-compatible in addition to being MR-safe, its presence and/or operation must not significantly affect the quality of the MR images and, inversely, its operation is not affected by the MR scanner. It is necessary that testing results related to MR compatibility and safety for robotic-associated devices should be accompanied by the exact testing conditions (scanner type, field strength, exact position, etc.), since an object may exhibit different behavior under different MR conditions. The issues of MR compatibility and safety cover any device exposed to the MR environment, such as implants, cardiac pacemakers, and drug infusion pumps (Schueler et al. 1999). There have been several comprehensive reviews of MR compatibility of materials and of testing methodologies along with many relevant references (Schenck 1996; Schaefers and Melzer 2006).

The definitions of the compatibility and safety terms also evolve along with new developments, such as extending the use of the MR modality from diagnostics to interventions. A more explicit characterization has recently been introduced, along with the appropriate required labeling, to describe the safety of objects in the MR environment (Schaefers 2008): (i) An item is *MR-safe* if it poses no known hazards in all MR environments; (ii) an item is *MR-conditional* if it has been demonstrated to pose no known hazards in a specified MR environment with specified conditions of use; and (iii) an item is *MR-unsafe* if it is known to pose hazards in any MR environment.

5.4.2 Construction Materials, Actuators, and Sensors

Construction materials, sensors, and actuators must be MR-compatible and adequate shielding of electronics and cabling must be ensured. Materials commonly used for the construction of robotic and mechatronic devices are often ferromagnetic (e.g., carbon steel) and/or conductive (e.g., aluminum). Ferromagnetic materials are not suitable for MR robotics. In general, conductive materials are also not compatible with the MR environment because the scanner's fast-switching magnetic fields and RF pulses may induce eddy currents that can be highly disruptive to imaging (Moscatel et al. 1995; Keeler et al. 1998; Shellock and Shellock 1998; Shellock 2000; Shellock and Crues 2004). These currents can also result in unwanted heating of devices or interventional tools that contain conductive elements such as needles and catheters, resulting in burns suffered by the patient (Shellock 2000; Dempsey et al. 2001).

Materials suitable for MR-compatible devices are non-magnetic and nonconductive, such as plastics, nylon, wood, silicone, ceramics, fiberglass, carbon fiber, and other composites, all of which have been extensively used for the development of MR compatible systems. Some of these materials have limited structural rigidity and that is reflected on the overall stiffness and manipulability of the device, as well as its ability to apply force. Limited metallic parts have sometimes been incorporated into otherwise MR-compatible mechatronic devices, including joining and transmission elements [e.g., Masamune et al. (1995); Kaiser et al. (2000); Susil et al. (2003)]. MR compatibility examinations often confirm that the presence of small metallic parts may not present substantial safety or compatibility concerns as long as their use is limited and they are placed adequately far away from the imaged area; also, any small magnetic part must be securely attached to a firm structure.

Standard actuators used in conventional mechatronics applications are not, in general, suitable for MR-compatible interventional systems, because either of their principle of operation or their construction materials. Standard electromagnetic motors and their drivers, for example, are constructed of metallic materials, and noise from their operation is likely to interfere with the MR image acquisition process. Perhaps the simplest alternative is to move and activate the interventional device manually, as with a system dedicated to prostate-related procedures (Susil et al. 2003; Krieger et al. 2005).

Hydraulics is also a possibility, but cylinders as well as the rest of the circuit components and the working fluid must be MR-compatible, and must not leak. This form of actuation has been implemented on a six-DOF manipulator for use in minimally invasive liver surgery performed inside open MR scanners (Kim et al. 2002). The use of a hydraulic master-slave system for MRI-related applications has been investigated in (Moser et al. 2003), with a focus on the dynamics of the system.

Pneumatics provides a cleaner form of actuation. The principle of operation is similar to hydraulics, based on the cylinder/piston arrangement, but the working fluid is air. Pneumatics systems typically operate at speeds higher than those of hydraulics, but they have limited stiffness and are suitable only for low-force applications, because of the compressibility of air. Specially developed pneumatic actuators are used with the commercial Innomotion™ system (Innomedic GmbH, Herxheim, Germany). Another example of pneumatic actuation is the PneuStep (Muntener et al. 2006; Stoianovici et al. 2007), which uses a stepper motor principles to achieve controllable precise motion.

A popular form of actuation with many of the systems developed to date has been with ultrasonic, piezoelectric motors (USM) (Masamune et al. 1995; Chinzei et al. 2000; Kaiser et al. 2000; Tsekos et al. 2001, 2005; Koseki et al. 2002). These motors are immune to the scanner magnetic fields, and they do not produce any magnetic fields themselves. Studies regarding their MR-compatibility characteristics were carried out by Chinzei et al. (1999). Favorable features of USM include high torque-to-weight ratio, small size, and compact shape, and they display a high breaking torque when not being actuated, which allows locking to their current position. There should be provisions for emergency situations such as power failures, however, in which case the system may have to be moved manually. Manually operated mechanical clutches, for example, could be installed to disengage the motor when required, effectively isolating it from the rest of the motion system [as example shown in Koseki et al. (2002)].

A defining factor of the MR-compatibility of an actuator is its physical placement relative to the scanner. USMs on mechatronic devices, for example, must be placed outside the scanner and at a sufficient distance from the imaging region; a transmission system can then convey motions to the distant actuated joints of the device with shafts, belts, cables, or linkages (Chinzei et al. 2000; Tsekos et al. 2001, 2005;

Koseki et al. 2002). Performance may be limited by the joint flexibility, backlash, and friction problems inherent in motion transmission systems, as discussed in Christoforou and Tsekos (2006).

Appropriate *sensing* technologies are also required for MR-compatible devices. Fiber-optics has received considerable attention for this purpose, for example in custom-designed incremental encoders for measurement of translational and rotational motions (Chinzei et al. 2000). As with standard optical encoders, glass grating patterns are used in sensing motion; fiber-optic cables transfer the signals to and from the optical components and circuitry, which are at a large distance from the scanner.

Fiber-optics has also been exploited for MR-compatible force sensing (Takahashi et al. 2003; Tada and Kanade 2004; Gassert et al. 2006). In one approach, light is sent along one fiber optic cable, and directed through a remotely located MR-compatible sensing element; after that, it travels back from the far side of the element to the rest of the optical system through a return cable. A physical displacement of the sensing element following the application of a force affects the passage of the light through it, i.e., between the two cables; comparison of the intensity of the transmitted and returning light yields the magnitude of the applied force. In a similar implementation, light from an emitting fiber is shone onto a mirror-type force sensor. Applied forces deform the sensing element and change the angle of the mirror, which affects the intensity of the light passing back through the receiving fiber. As a result, the amount of returning light can be directly correlated to the applied force (Gassert et al. 2006). The main advantage of this approach over the "through-beam" arrangement is sensor compactness, given that both fiber optic cables connect on the same side of the sensor.

5.5 Robotic Manipulators for MRI-Guided Interventions

In this section we will review some of the major developments that illustrate the innovations in a wide range of fields, such as mechanical design and prototyping, actuation, non-MR–based sensing, image guidance, MR methodology, and system integration. In general, with the current status of the technology, robotic devices can perform only part of a procedure, such as positioning, maneuvering, and inserting a probe. In a brain biopsy, for example, a craniotomy must be performed prior to commencing the robot-assisted tasks, at present, and an incision is needed before a breast intervention. The technologies reviewed below, however, may enable multi-tasking systems that can assist in a wider range of tasks.

One of the first MR-compatible robotic systems (Masamune et al. 1995) was a needle insertion manipulator for stereotactic neurosurgical applications. This six-DOF manipulator was actuated by ultrasonic motors and was directly mounted on the patient couch. Among the challenges that this pioneering work revealed was the limited stiffness of MR-compatible parts made of nonmetallic materials, which affected the accuracy of the device. On a system developed for use with a unique 0.5 T double-donut MR scanner (Chinzei et al. 2000; Chinzei and Miller 2001), the actuation assembly is mounted on an overhead structure, and two long rigid arms extend into the gap between the two halves of the magnet. The system is constructed of paramagnetic materials, with the rigid arms reaching inside the imaging volume made of a titanium alloy. With five available DOFs and actuated with ultrasonic motors, the system can position and direct an axially symmetric interventional tool. Given this arrangement the bulky actuation assembly does not obstruct the access of the physician to the patient, and placement of the motors away from the imaging volume reduces MR-compatibility issues.

A system for MRI-guided manipulation of endoscopes, with a particular focus on trans-nasal neurosurgical procedures, combines the limited keyhole-like perception offered by an endoscope with 3D volumetric MR vision (Koseki et al. 2002). The robotic component of this system has four DOFs, and is actuated with ultrasonic motors. Studies performed to assess the accuracy and stiffness of the system at a 0.3 T open scanner demonstrated that, while the deployment of the manipulator did not affect the quality of the images, the activation of the motors was causing excessive noise. As a result, imaging was limited to times when the motors were not actuated, an approach also adopted by other researchers.

A high-accuracy system has been developed for prostate interventions, such as needle biopsy, fiducial marker placement, injections in the prostate, and delivery of localized therapy (Susil et al. 2003, 2004). It is constructed mainly of plastic materials, along with a few small metallic parts, and includes miniature MR markers attached to the end-effector to track it (Table 5–2). Although it was manually actuated from outside the bore, it is a great demonstration of a mechanical design adapted to a particular anatomy. A more recent, compact robotic system actuated with USMs was designed for prostate interventions inside closed bore scanners (Goldenberg et al. 2008), and is mounted on the table in between the patient's legs.

Breast MRI is an excellent candidate for combination with robotics, especially for biopsies. The first such breast-specific system was the ROBITOM, which is actuated with USMs and operates inside cylindrical scanners (Kaiser et al. 2000). This system was used for one of the first MRI-guided robotic interventions on patients at 1.5 T (Pfleiderer et al. 2003), and it led to an improved version (Pfleiderer et al. 2005). ROBITOM II incorporates a system for high-speed needle insertion to improve targeting accuracy by effectively minimizing lesion shifting, along with a specially designed double breast biopsy coil to improve images and access to the breasts. Both phantom and human studies have demonstrated successful harvesting of biopsy samples. Another MR-compatible system for breast applications was developed by Tsekos et al. (2001) and improved by Larson et al. (2004). That experimental five-DOF system offers the unique feature of access to the breast with practically any desired orientation. This system employs USMs located away from the imaged area and a transmission system of shafts and universal joints. Experimental studies on breast phantoms were performed inside a 4 T scanner.

Investigators have explored a variety of application-specific MR-compatible robots. The operation of an MRI-guided microwave thermotherapy system for liver tumors (Hata et al. 2005), for example, is based on a "remote center of motion" approach, with a three-DOF Cartesian motion stage that carries a needle holder with unconstrained two-DOF rotation. The system is placed on the side of the bed and aluminum is the main construction material.

Another prototype robot with unique kinematic design consists of two six-DOF robotic manipulators with interchangeable surgical tools, to be used with the all-around open scanners (Tajima et al. 2004). The system is controlled in master-slave mode, in which the operator maneuvers a pair of control handles (master manipulators) on the control device and the actual arms (slave manipulators) precisely replicate that motion.

The "Light Puncture Robot" is another new robotic system with a unique body-supported architecture that allows it to passively follow the surface motion of the body with respiration or other patient movements (Bricault et al. 2008). It is constructed of lightweight plastic materials, uses specially developed pneumatic actuators, and can be used with both MRI and CT.

One of the few commercially available MR-compatible interventional robotic systems is the Innomotion™ (Innomedic GmbH, Herxheim, Germany) (Cleary et al. 2006; Jantschke et al. 2007; Zangos et al. 2007; Li et al. 2008; Melzer et al. 2008). Its five-DOF robotic arm is designed specifically to assist in MRI-guided percutaneous interventions, such as spinal procedures for pain therapy, tumor therapy, and biopsies. The arm is attached to an arc-shaped support base (orbit ring) mounted on the patient's couch, and it can be prepositioned onto the orbit ring at certain locations, depending on the required access to the patient. Its operation is based on pneumatic actuators and optical sensors. Several studies with the system have been reported including an animal study of image-guided targeting inside a 1.5 T cylindrical scanner (Hempel et al. 2003; Bock et al. 2005).

NeuroArm, an MR-guided device designed for neurosurgical applications, has two anthropomorphic arms, each with seven DOFs, that can maneuver microsurgical tools (Sutherland et al. 2008; Pandya et al. 2009). The two arms are controlled in a master/slave mode, and operated through a workstation using real-time MR images. Haptic interfaces provide the operator with force feedback information obtained from 3D force sensors on the end-effector. An important feature is that the system can filter out hand tremor. The main construction materials are titanium and polyetheretherketone (PEEK), and actuation is by way of ultrasonic piezoelectric motors.

5.6 Concluding Remarks

The aforediscussed innovative studies demonstrate the technical feasibility of combining robotics and MRI guidance. The versatility and robustness of the MR modality (reviewed in Tables 5–1 and 5–2), enhanced by the extensive experience and talent accumulated in the field, have resulted in an ever-growing wealth of technological and methodological advancements. We therefore may claim, with reasonable confidence, that the modality is mature enough to meet most needs in MRI-guided robot-assisted interventions.

It is the clinical merit of the technology, of course, that will determine its further evolution and eventual fate (Tsekos et al. 2008). MRI-guided robot-assisted procedures will have to offer substantial improvements in patient management, compared to current interventional practices, or facilitate new procedures not otherwise possible. Potential clinical benefits of the approach, however, are easy to imagine. Several technical challenges do remain in the areas of mechatronics and system integration. One of these is the need to develop highly reliable actuators and non-MR–based sensing technologies. Another is the incorporation of haptic interfaces to provide the operator with tactile feedback information. These and the other technical difficulties that have been identified, however, appear to be resolvable.

But the need for further technical innovations and assessment of clinical merit offer medical physicists, biomedical engineers, and interventionalists, surgeons, and other physicians unique opportunities to contribute to this exciting and highly promising technology of the future.

5.7 Acknowledgments

The authors would like to thank Profs. Andrew Karellas and Anthony B. Wolbarst for their editorial comments. This work was supported in part by the National Science Foundation grant CNS-0932272 entitled "CPS: Medium: Image Guided Robot-Assisted Medical Interventions," HEAF 97722, and the Cyprus Research Promotion Foundation TECH/MECH/0308(BIE)/05. All opinions, findings, conclusions or

recommendations expressed in this work are those of the authors and do not necessarily reflect the views of our sponsors.

5.8 References

Anderson, C. A., A. P. Kypson, and W. R. Chitwood, Jr. (2008). "Robotic mitral surgery: Current and future roles." *Curr Opin Cardiol* 23(2):117–120.

Atalar, E., D. L. Kraitchman, B. Carkhuff, J. Lesho, O. Ocali, M. Solaiyappan, M. A. Guttman, and H. K. Charles, Jr. (1998). "Catheter-tracking FOV MR fluoroscopy." *Magn Reson Med* 40(6):865–872.

Bock, M., A. Melzer, H. Bardenheuer, H. Ghaderi, B. Gutmann, H. Zimmermann, and W. Semmler. "MR-Guided Percutaneous Interventions Using a Robotic Assistance System: Initial Experiences in a Pig Model." International Society of Magnetic Resonance in Medicine, Miami, FL, 2005.

Boyd, W. D., K. Kodera, K. D. Stahl, and R. Rayman. (2002). "Current status and future directions in computer-enhanced video- and robotic-assisted coronary bypass surgery." *Semin Thorac Cardiovasc Surg* 14(1):101–109.

Bricault, I., N. Zemiti, E. Jouniaux, C. Fouard, E. Taillant, F. Dorandeu, and P. Cinquin. (2008). "Light puncture robot for CT and MRI interventions: Designing a new robotic architecture to perform abdominal and thoracic punctures." *IEEE Eng Med Biol Mag* 27(3):42–50.

Chinzei, K., and K. Miller. "MRI Guided Surgical Robot" In: Proceedings of the Australian Conference on Robotics and Automation, Sydney, 2001. Heidelberg: Springer, 2001.

Chinzei, K., R. Kikinis and F. A. Jolesz. "MR Compatibility of Mechatronic Devices: Design Criteria" In: *Medical Image Computing and Computer-Assisted Intervention.* Cambridge, UK: Springer, 1999.

Chinzei, K., N. Hata, F. Jolesz, and R. Kikinis. "MR Compatible Surgical Assist Robot: System Integration and Preliminary Feasibility Study." In: Proceedings of the Medical Image Computing and Computer-Assisted Intervention, Pittsburgh, PA, 2000. New York: Springer, 2000.

Christoforou, E., and N. V. Tsekos. "Robotic Manipulators with Remotely-Actuated Joints: Implementation Using Drive Shafts and U-Joints" In: Proceedings of the IEEE International Conference on Robotics and Automation, Orlando, FL, pp. 2886–2871, 2006.

Christoforou, E., E. Akbudak, A. Ozcan, M. Karanikolas, and N. V. Tsekos. (2007). "Performance of interventions with manipulator-driven real-time MR guidance: implementation and initial in vitro tests." *Magn Reson Imaging* 25(1):69–77.

Cleary, K., A. Melzer, V. Watson, G. Kronreif, and D. Stoianovici. (2006). "Interventional robotic systems: Applications and technology state-of-the-art." *Minim Invasive Ther Allied Technol* 15(2):101–113.

Debatin, J. F., A. Gerhard, A. L. Braert, and R. W. Günther. *Interventional Magnetic Resonance Imaging*. Heidelberg: Springer, 1998.

Dempsey, M. F., B. Condon, and D. M. Hadley. (2001). "Investigation of the factors responsible for burns during MRI." *J Magn Reson Imaging* 13(4):627–631.

FDA. U.S. Food and Drug Administration and CDRH Magnetic Resonance Working Group. (1997). "A Primer on Medical Device Interactions with Magnetic Resonance Imaging Systems." http://fda.gov/MedicalDevices/DeviceRegulationandGuidance/GuidanceDocuments/ucm107721.htm. Accessed May 2010.

Felden, A., J. Vagner, A. Hinz, H. Fischer, S. O. Pfleiderer, J. R. Reichenbach, and W. A. Kaiser. (2002). "ROBITOM-robot for biopsy and therapy of the mamma." *Biomed Tech (Berl)* 47(Suppl 1 Pt 1):2–5.

Gassert, R., R. Moser, E. Burdet, and K. Chinzei. (2006). "MRI/fMRI-compatible robotic system with force feedback for interaction with human motion." *IEEE/ASME Trans Mechatronics* 11(2):216–224.

Gassert, R., E. Burdet, and K. Chinzei. (2008a). "MRI-Compatible robotics." *IEEE Eng Med Biol Mag* 27(3):12–14.

Gassert, R., E. Burdet, and K. Chinzei. (2008b). "Opportunities and challenges in MR-compatible robotics: Reviewing the history, mechatronic components, and future directions of this technology." *IEEE Eng Med Biol Mag* 27(3):15–22.

Goh, P., Y. Tekant, and S. M. Krishnan. (1993). "Future developments in high-technology abdominal surgery: Ultrasound, stereo imaging, robotics." *Baillieres Clin Gastroenterol* 7(4): 961–987.

Goldenberg, A. A., J. Trachtenberg, W. Kucharczyk, Y. Yi, M. Haider, L. Ma, R. Weersink, and C. Raoufi. (2008). "Robotic system for closed-bore MRI-guided prostatic interventions." *IEEE/ASME Trans Mechatronics* 13:374–379.

Hata, N., R. Hashimoto, J. Tokuda, and S. Morikawa. "Needle Guiding Robot for MR-Guided Microwave Thermotherapy of Liver Tumor Using Motorized Remote-Center-of-Motion Constraint." In: Proceedings of the IEEE Internation Conference on Robotics and Automation, Barcelona, Spain, 2005.

Hempel, E., H. Fischer, L. Gumb, T. Hohn, H. Krause, U. Voges, H. Breitwieser, B. Gutmann, J. Durke, M. Bock, and A. Melzer. (2003). "An MRI-compatible surgical robot for precise radiological interventions." *Comput Aided Surg* 8(4):180–191.

Hillenbrand, C. M., D. R. Elgort, E. Y. Wong, A. Reykowski, F. K. Wacker, J. S. Lewin, and J. L. Duerk. (2004). "Active device tracking and high-resolution intravascular MRI using a novel catheter-based, opposed-solenoid phased array coil." *Magn Reson Med* 51(4):668–675.

Jantschke, R., T. Haas, P. Madoerin, and S. Dziergwa. (2007). "Preparation, assistance and imaging protocols for robotically assisted MR and CT-based procedures." *Minim Invasive Ther Allied Technol* 16(4):217–221.

Jolesz, F. A., R. Kikinis, and I. F. Talos. (2001). "Neuronavigation in interventional MR imaging. Frameless stereotaxy." *Neuroimaging Clin N Am* 11(4):685–693, ix.

Jolesz, F. A., P. R. Morrison, S. J. Koran, R. J. Kelley, S. G. Hushek, R. W. Newman, M. P. Fried, A. Melzer, R. M. Seibel, and H. Jalahej. (1998). "Compatible instrumentation for intraoperative MRI: Expanding resources." *J Magn Reson Imaging* 8(1): 8–11.

Jolesz, F. A., A. Nabavi, and R. Kikinis. (2001). "Integration of interventional MRI with computer-assisted surgery." *J Magn Reson Imaging* 13(1):69–77.

Kaiser, W. A., H. Fischer, J. Vagner, and M. Selig. (2000). "Robotic system for biopsy and therapy of breast lesions in a high-field whole-body magnetic resonance tomography unit." *Invest Radiol* 35(8):513–519.

Karanikolas, M., E. Christoforou, E. Akbudak, P. E. Eisebeis, and N. V. Tsekos. "An Archetype for MRI Guided Tele-interventions" In: *Artificial Intelligence Applications and Innovations*. Boston: Springer: International Federation for Information Processing, pp. 476–483, 2006.

Karmarkar, P. V., D. L. Kraitchman, I. Izbudak, L. V. Hofmann, L. C. Amado, D. Fritzges, R. Young, M. Pittenger, J. W. Bulte, and E. Atalar. (2004). "MR-trackable intramyocardial injection catheter." *Magn Reson Med* 51(6):1163–1172.

Keeler, E. K., F. X. Casey, H. Engels, E. Lauder, C. A. Pirto, T. Reisker, J. Rogers, D. J. Schaefer, and T. Tynes. (1998). "Accessory equipment considerations with respect to MRI compatibility." *J Magn Reson Imaging* 8(1):12–18.

Kim, D., E. Kobayashi, T. Dohi, and I. Sakuma. "A New, Compact MR-Compatible Surgical Manipulator for Minimally Invasive Liver Surgery." Medical Image Computing and Computer-Assisted Intervention, Tokyo, Japan, 2002.

Koseki, Y., T. Washio, K. Chinzei, and H. Iseki. "Endoscope Manipulator for Trans-Nasal Neurosurgery, Optimized for and Compatible to Vertical Field Open MRI." Proceedings of Medical Image Computing and Computer-Assisted Intervention, Tokyo, Japan. Heidelberg: Springer, 2002.

Krieger, A., R. C. Susil, C. Menard, J. A. Coleman, G. Fichtinger, E. Atalar, and L. L. Whitcomb. (2005). "Design of a novel MRI compatible manipulator for image guided prostate interventions." *IEEE Trans Biomed Eng* 52(2):306–313.

Larson, B. T., A. G. Erdman, N. V. Tsekos, E. Yacoub, P. V. Tsekos, and I. G. Koutlas. (2004). "Design of an MRI-compatible robotic stereotactic device for minimally invasive interventions in the breast." *J Biomech Eng* 126(4):458–465.

Li, M., D. Mazilu, and K. A. Horvath. (2008). "Robotic System for Transapical Aortic Valve Replacement with MRI Guidance." *Med Image Comput Comput Assist Interv* 11(Pt 2): 476–484.

Lufkin, R. B. (ed.). *Interventional MRI*. St. Louis: Mosby, 1999.

Masamune, K., E. Kobayashi, Y. Masutani, M. Suzuki, T. Dohi, H. Iseki, and K. Takakura. (1995). "Development of an MRI-compatible needle insertion manipulator for stereotactic neurosurgery." *J Image Guid Surg* 1(4):242–248.

Melzer, A., B. Gutmann, T. Remmele, R. Wolf, A. Lukoscheck, M. Bock, H. Bardenheuer, and H. Fischer. (2008). "INNOMOTION for percutaneous image-guided interventions: principles and evaluation of this MR- and CT-compatible robotic system." *IEEE Eng Med Biol Mag* 27(3):66–73.

Menciassi, A., M. Quirini, and P. Dario. (2007). "Microrobotics for future gastrointestinal endoscopy." *Minim Invasive Ther Allied Technol* 16(2):91–100.

Moscatel, M. A., F. G. Shellock, and S. M. Morisoli. (1995). "Biopsy needles and devices: assessment of ferromagnetism and artifacts during exposure to a 1.5-T MR system." *J Magn Reson Imaging* 5(3):369–372.

Moser, R., R. Gassert, E. Burdet, L. Sache, H. R. Woodtli, J. Erni, W. Maeder, and H. Bleuler. "An MR Compatible Robot Technology," In: Proceedings of the IEEE International Conference on Robotics and Automation, 2003.

Muntener, M., A. Patriciu, D. Petrisor, D. Mazilu, H. Bagga, L. Kavoussi, K. Cleary, and D. Stoianovici. (2006). "Magnetic resonance imaging compatible robotic system for fully automated brachytherapy seed placement." *Urology* 68(6): 1313–1317.

Nathoo, N., M. Vogelbaum, and G. Barnett. (2005). "In touch with robotics: Neurosurgery for the future." *Neurosurgery* 56(3): 421–433.

Ozcan, A., E. Christoforou, D. Brown, and N. Tsekos. (2006). "Fast and efficient radiological interventions via a graphical user interface commanded magnetic resonance compatible robotic device." *Conf Proc IEEE Eng Med Biol Soc* 1:1762–1767.

Ozcan, A., and N. V. Tsekos. (2008). "The interconnection of MRI scanner and MR compatible robotic device: Synergistic graphical user interface to form a mechatronic system." *IEEE/ASME Trans Mechatronics* 13(3):362–369.

Pandya, S., J. W. Motkoski, C. Serrano-Almeida, A. D. Greer, I. Latour, and G. R. Sutherland. (2009). "Advancing neurosurgery with image-guided robotics." *J Neurosurg* 111(6): 1141–1149.

Pfleiderer, S. O., C. Marx, J. Vagner, R. P. Franke, J. R. Reichenbach, and W. A. Kaiser. (2005). "Magnetic resonance-guided large-core breast biopsy inside a 1.5-T magnetic resonance scanner using an automatic system: In vitro experiments and preliminary clinical experience in four patients." *Invest Radiol* 40(7):458–463.

Pfleiderer, S. O., J. R. Reichenbach, T. Azhari, C. Marx, A. Malich, A. Schneider, J. Vagner, H. Fischer, and W. A. Kaiser. (2003). "A manipulator system for 14-gauge large core breast biopsies inside a high-field whole-body MR scanner." *J Magn Reson Imaging* 17(4):493–498.

Reijnen, M. M., C. J. Zeebregts, and W. J. Meijerink. (2005). "Future of operating rooms." *Surg Technol Int* 14:21–27.

Schaefers, G. (2008). "Testing MR safety and compatibility." *IEEE Eng Med Biol Mag* 27(3):23–27.

Schaefers, G., and A. Melzer. (2006). "Testing methods for MR safety and compatibility of medical devices." *Minim Invas Ther Allied Technol* 15(2):71–75.

Schenck, J. F. (1996). "The role of magnetic susceptibility in magnetic resonance imaging: MRI magnetic compatibility of the first and second kinds." *Med Phys* 23(6):815–850.

Schenck, J. F. (1998). "MR safety at high magnetic fields." *Magn Reson Imaging Clin N Am* 6(4):715–730.

Schenck, J. F. (2000). "Safety of strong, static magnetic fields." *J Magn Reson Imaging* 12(1):2–19.

Schueler, B. A., T. B. Parrish, J.-C. Lin, B. E. Hammer, B. J. Pangrle, E. R. Ritenour, J. Kucharczyk, and C. L. Truwit. (1999). "MRI compatibility and visibility assessment of implantable medical devices." *J Magn Reson Imaging* 9(4):596–603.

Shellock, F. G. (2000). "Radiofrequency energy-induced heating during MR procedures: a review." *J Magn Reson Imaging* 12(1):30–36.

Shellock, F. G., and J. V. Crues. (2004). "MR procedures: Biologic effects, safety, and patient care." *Radiology* 232(3):635–652.

Shellock, F. G., and V. J. Shellock. (1998). "Cardiovascular catheters and accessories: ex vivo testing of ferromagnetism, heating, and artifacts associated with MRI." *J Magn Reson Imaging* 8(6):1338–1342.

Stoianovici, D., A. Patriciu, D. Petrisor, D. Mazilu, and L. R. Kavoussi. (2007). "Pneumatic step motor." *IEEE/ASME Trans Mechatronics* 12(1):98–106.

Susil, R. C., K. Camphausen, P. Choyke, E. R. McVeigh, G. S. Gustafson, H. Ning, R. W. Miller, E. Atalar, C. N. Coleman, and C. Menard. (2004). "System for prostate brachytherapy and biopsy in a standard 1.5 T MRI scanner." *Magn Reson Med* 52(3):683–687.

Susil, R. C., A. Krieger, J. A. Derbyshire, A. Tanacs, L. L. Whitcomb, G. Fichtinger, and E. Atalar. (2003). "System for MR image-guided prostate interventions: canine study." *Radiology* 228(3):886–894.

Sutherland, G. R., I. Latour, and A. D. Greer. (2008). “Integrating an image-guided robot with intraoperative MRI: A review of the design and construction of neuroArm.” *IEEE Eng Med Biol Mag* 27(3):59–65.

Tada, M., and T. Kanade. “Development of an MR-Compatible Optical Force Sensor,” In: Proceedings of the International Conference of the IEEE EMBS, San Francisco, CA, 2004.

Tajima, F., K. Kishi, K. Nishizawa, K. Kan, H. Ishii, K. Sudo, M. G. Fujie, and T. Dohi. “A Prototype Master-Slave System Consisting of Two MR-Compatible Manipulators with Interchangeable Surgical Tools.” IEEE International Conference on Robotics and Automation, New Orleans, LA, 2004.

Takahashi, N., M. Tada, J. Ueda, Y. Matsumoto, and T. Ogasawara. “An Optical 6-Axis Force Sensor for Brain Function Analysis Using fMRI.” IEEE International Conference on Sensors, Toronto, ON, Canada, 2003.

Taylor, G. W., and D. G. Jayne. (2007). “Robotic applications in abdominal surgery: their limitations and future developments.” *Int J Med Robot* 3:3–9.

Tsekos, N. V., E. Christoforou, and A. Ozcan. (2008). “A general-purpose MR-compatible robotic system: implementation and image guidance for performing minimally invasive interventions.” *IEEE Eng Med Biol Mag* 27(3):51–58.

Tsekos, N. V., A. Khanicheh, E. Christoforou, and C. Mavroidis. (2007). “Magnetic resonance-compatible robotic and mechatronics systems for image-guided interventions and rehabilitation: A review study.” *Annu Rev Biomed Eng* 9:351–387.

Tsekos, N. V., A. Ozcan, and E. Christoforou. (2005). “A prototype manipulator for magnetic resonance-guided interventions inside standard cylindrical magnetic resonance imaging scanners.” *J Biomech Eng* 127(6):972–980.

Tsekos, N. V., A. Ozcan, and E. Christoforou. (2005). “A prototype manipulator for MR-guided interventions inside standard cylindrical MRI scanners.” *J Biomech Eng* 127:972–980.

Tsekos, N. V., J. Shudy, E. Yacoub, P. V. Tsekos, and I. G. Koutlas. “Development of a Robotic Device for MRI-Guided Interventions in the Breast. 2nd IEEE International Symposium on Bioinformatics and Bioengineering, Washington, DC, 2001.

Wacker, F. K., C. M. Hillenbrand, J. L. Duerk, and J. S. Lewin. (2005). “MR-guided endovascular interventions: Device visualization, tracking, navigation, clinical applications, and safety aspects.” *Magn Reson Imaging Clin N Am* 13(3):431–439.

Zangos, S., C. Herzog, K. Eichler, R. Hammerstingl, A. Lukoschek, S. Guthmann, B. Gutmann, U. J. Schoepf, P. Costello, and T. J. Vogl. (2007). “MR-compatible assistance system for punction in a high-field system: device and feasibility of transgluteal biopsies of the prostate gland.” *Eur Radiol* 17(4):1118–1124.

Zhang, Q., M. Wendt, A. J. Aschoff, L. Zheng, J. S. Lewin, and J. L. Duerk. (2000). “Active MR guidance of interventional devices with target-navigation.” *Magn Reson Med* 44(1):56–65.

Zhang, Q., M. Wendt, A. J. Aschoff, J. S. Lewin, and J. L. Duerk. (2001). “A multielement RF coil for MRI guidance of interventional devices.” *J Magn Reson Imaging* 14(1):56–62.